CLINICAL AND EXPERIMENTAL
OPTOMETRY

INVITED REVIEW

Correction of presbyopia: old problems with old (and new) solutions

Clin Exp Optom 2020; 103: 21–30 DOI:10.1111/cxo.12987

Pete S Kollbaum OD PhD FAAO
Arthur Bradley PhD
School of Optometry, Indiana University, Bloomington, Indiana, USA
E-mail: kollbaum@indiana.edu

Submitted: 13 July 2019
Revised: 5 September 2019
Accepted for publication: 20 September 2019

We live in a three-dimensional world and the human eye can focus images from a wide range of distances by adjusting the power of the eye's lens (accommodation). Progressive senescent changes in the lens ultimately lead to a complete loss of this ability by about age 50, which then requires alternative strategies to generate high-quality retinal images for far and close viewing distances. This review paper highlights the biomimetic properties and underlying optical mechanisms of induced anisometropia, small apertures, dynamic lenses, and multi-optic lenses in ameliorating the visual consequences of presbyopia. Specifically, the advantages and consequences of non-liner neural summation leveraged in monovision treatments are reviewed. Additionally, the value of a small pupil is quantified, and the impact of pinhole pupil location and their effects on neural sensitivity are examined. Different strategies of generating multifocal optics are also examined, and specifically the interaction between ocular and contact or intraocular lens aberrations and their effect on resulting image quality are simulated. Interestingly, most of the novel strategies for aiding presbyopic and pseudophakic eyes (for example, monovision, multifocality, pinhole pupils) have emerged naturally via evolution in a range of species.

Key words: accommodation, anisometropia, aspheric, multifocal, presbyopia, pupil, spherical aberration

We live in a three-dimensional world, and with monofocal optics, only one object distance can generate a focused image at any given time.[1,2] Therefore, most of the retinal image is likely to be out of focus most of the time. However, optical defocus can be catastrophic for human vision[3] and may also be a stimulus for failed emmetropisation and the continued eye growth that underlies myopia.[4–6]

Most vertebrate eyes focus images on the retina by adjusting the optical power of the eye as stimulus distance changes by either moving the eye's lens (for example, fish[7–9] and cats[10]), adjusting the power of the eye's lens (for example, humans), or adjusting the power of the cornea (for example, chameleons).[11–13] However, less common strategies are employed that use a pinhole pupil to expand the depth of field (for example, nautilus[14]), multifocal optics (for example, fish[15]), and different powers in different eyes (for example, chameleons[16]). Variants of these less common strategies are now being utilised by older humans who have lost the ability to adjust power of their lenses (presbyopes and pseudphakes[17,18]), a senescent trait also observed in non-human primates and other mammals.[18,19] This paper builds upon recent comprehensive reviews[20,21] to examine the optical implications of current and potential strategies to focus the retinal image despite the loss of accommodative ability.

Induced anisometropia

Although different distances can be focused by employing different optical powers in each eye (for example, chameleons[16]), evolution has not developed this approach for humans for whom anisometropia is rare and a possible cause of visual cortical disruption if present in early life (amblyopia, loss of stereopsis).[22] However, inducing anisometropia in older presbyopic or pseudophakic patients ('monovision') has been shown to expand the binocular depth of field by generating clear bifocality of the binocular visual system,[23–26] and high-quality vision at two distances (Figure 1).[27] The success of monovision hinges on the observation that vision with one focused and one defocused eye is dominated by the focused image,[28] as shown quantitatively in studies of contrast sensitivity[23–25] and visual acuity.[26,29] The improvement in near vision created by correcting one eye can be dramatic, but monovision does not replicate the range of high-quality vision observed in young adults (Figure 1). There is a small reduction of peak acuity and contrast sensitivity down to levels observed with monocular vision.[30,31] Additionally, intermediate distance vision (where neither eye has a focused image) is significantly degraded, an effect that is exacerbated by high add powers[23,26] (Figure 1). Also, because monocular defocus is especially detrimental to stereopsis,[32,33] patients fit with monovision corrections have compromised stereo acuity[34,35] and discrimination of suprathreshold horizontal disparities.[36] Furthermore, in binocularly vulnerable patients monovision can induce strabismus.[37]

Unlike a bifocal lens which simultaneously produces focused and defocused images that add optically (and therefore linearly) at the retina, a monovision patient must employ binocular neural summation to add focused and defocused images in the cortex where non-linear summation[38] or cross-eye neural inhibition[39] is thought to reduce the visibility of the defocused image.[28]

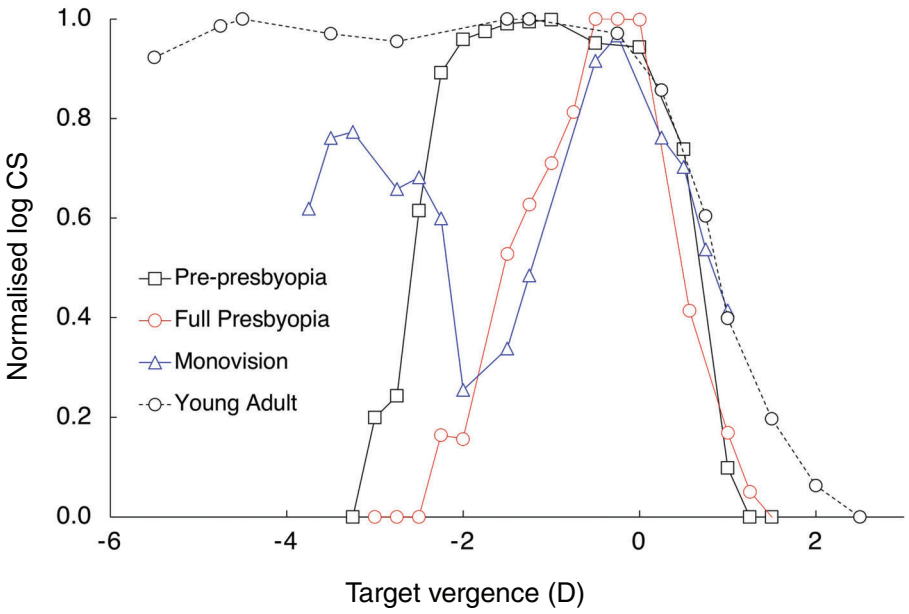

Figure 1. Contrast sensitivity plotted as a function of target vergence (dioptres) for four different subjects: A young adult (24 years of age; circle symbols and black dashed line), a pre-presbyope not yet requiring a reading add (44 years of age; square symbols and black solid line), a full presbyope who had been using a reading add for several years (44 years of age; red circle symbols and red solid line), and a full presbyope wearing a +3.00 D add in front of one eye (blue triangle symbols and blue solid line). Y-axis is log normalised CS (log CS/best corrected binocular single vision log contrast sensitivity).

Small aperture optics

The need for multiple optical powers can be avoided by employing pinhole optics, which can expand the depth of field of the eye[21,40,41] because the blur resulting from defocus is approximately proportional to pupil diameter.[42] The invertebrate nautilus employs this type of pinhole eye design, achieving imaging and depth of field with a small pupil,[14] and to a lesser extent, there is some argument that human vision also employs this small pupil strategy. Pupil size generally decreases over the age of 50,[43] and the retention of near vision pupil miosis in older eyes[44,45] can further reduce pupil size for the near viewing conditions where defocus is more likely. The smaller pupils in older eyes effectively correct for the increased aberrations found in these eyes.[46,47] However, the senescent decrease in photopic and mesopic pupil diameters in 65 year old eyes (for example, ranging from 4.7 to 3.8 photopically and 6.8 to 4.9 mm mesopically[43]) fails to provide sufficient expansion of the depth of field for older observers, who typically require some optical correction to read at near.[48]

The impact of pupil size on depth of field can be seen in Figure 2 where image quality (visual Strehl ratio on optical transfer function)[49–51] is plotted as a function of target vergence (adapted from Xu et al.[41]) assuming high photopic light levels and a typically aberrated older eye. The depth of field versus diffraction blur trade-off can be seen. The impact of diffraction is striking once the pupil size is reduced to under 2 mm, and peak image quality for the 0.5 mm pupil is less than 10 per cent of that achieved with mid-sized pupils. However, for near distances between 100 and 50 cm, the 1 mm pupil provides the best image quality, and it outperforms the 0.5 mm pupil over more than a 3.5 D range. The degradation in image quality due to the added spherical aberration reduces peak image quality for the largest pupil (7 mm) to that observed with a 1 mm pupil. Maximum peak image quality is observed with pupil diameters between 2.5 and 4.5 mm. For this aberrated eye that is paraxially emmetropic, there is a small myopic shift as the pupil is dilated due to positive spherical aberration.

Clinical strategies that employ pinhole pupils to expand the eye's depth of field have a long history (for example, Daza de Valdes, 1591, cited in a recent review by Charman[21]). Three key parameters must be selected: pupil axial location, pupil size, and whether to employ a fixed pupil or one that varies with light level.

Small pupils have been introduced into the spectacle plane,[52–54] corneal plane[55,56] and iris plane.[57] Placing a small pupil into the spectacle plane will expand the eye's depth of field (as proposed by Donders), but will also drastically reduce the field of view (for example, a 1 mm pinhole placed 17 mm in front of the eye's entrance pupil will start vignetting the retinal image for field eccentricities of about +/–3 degrees),[52,53] which limits the clinical utility of such an approach. One strategy to deal with this field restriction has been to employ multiple pinholes in the spectacle plane, obtaining some depth of field expansion and each individual pinhole allowing light to reach the retina from different field locations producing a complex patchwork of images and scotomas.[53] Placing the pinhole into the corneal plane either surgically[58–60] or with a contact lens[61] reduces the field constriction effect. However, light from the mid-periphery will still be blocked from entering the eye,[62–66] and total peripheral field occlusion can only be avoided by employing an annular 'iris', which for large field angles allows light to enter the eye around the outside of the inlay.[63] These field constriction problems can be avoided by placing the pinhole pupil into or very close to the iris plane (for example, by employing pharmacological miotics),[67–70] or including a small aperture into the anterior surface of an intraocular lens (IOL),[55,57,71] or piggy-back implantation of a pinhole aperture.[72]

Selection of pinhole pupil size is affected by many factors, but a balance must be struck between improving the defocused near vision without compromising focused distance vision.[73] The value of pinhole optics for presbyopic vision occurs because blur resulting from defocus will approximately scale in proportion to the amount of defocus and pupil diameter,[42] for example, the blur present in the retinal image when a distance-corrected presbyope views a stimulus at 50 cm through a 6 mm pupil can be halved by adding a +1.00 D correcting lens, or reducing pupil diameter to 3 mm. However, this proportionality rule ignores the impact of diffraction and optical aberrations.

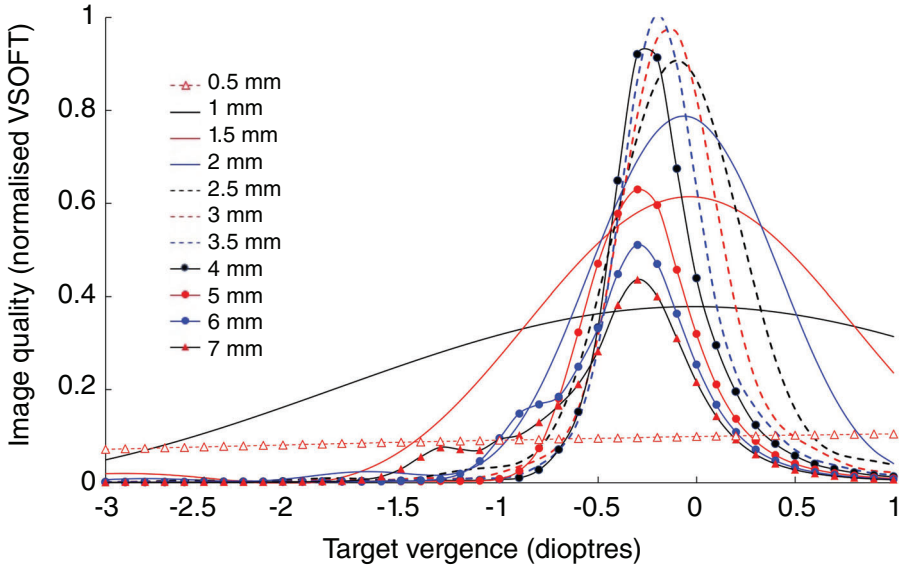

Figure 2. Image quality for different pupil diameters is plotted as a function of target vergence (dioptres) for a model eye with 0.2 microns of primary spherical aberration (C_4^0). Image quality is quantified by the visual Strehl ratio on optical transfer function metric[49–51] normalised to the diffraction limited value observed with a 3 mm diameter pupil.

It also fails to capture the significant impact of pupil constriction on retinal illuminance and vision.[73] As pupil size decreases, the role of diffraction blur in degrading image quality is amplified,[41] but the impact of higher-order aberrations is reduced, which produces a peak image quality in a focused eye for pupil diameters between 2 and 3 mm.[73,74] At high light levels, where Weber's law is effective, the accompanying drop in retinal illuminance produced by pupil constriction has no effect on vision.[75] However, at low photopic and mesopic light levels, reducing retinal illuminance lowers contrast sensitivity due to photon noise effects,[73,76] and the combined effects of diffraction and reductions in retinal illuminance can significantly impair distance vision when pupil diameters are decreased below 2.5 mm.[74] These studies emphasise that, as is the case for normal human vision,[77,78] the optimum pupil diameter for presbyopia treatment is larger at low environmental light levels.[74] Interestingly, in highly aberrated eyes, depth of focus can be expanded by either constricting the pupil (pinhole pupil effect) or dilating the pupil (multifocal optics effect).[41]

Pinhole spectacle devices have employed pupils less than 1 mm (for example, 0.9 mm[52,53]), with a resulting diffraction limit of < 30 cpd, which predictably impairs focused vision in the central field at photopic light levels.[53] For example, the KAMRA corneal inlays employ a 1.6 mm artificial pupil, which has proven effective at providing reading at near in photopic conditions.[60,79] Pharmacological pupil miotics have reduced pupil diameters to between 1–2 mm at photopic light levels, providing significant improved near vision and effective near reading.[68] However, laboratory studies reveal that such small pupils will significantly degrade focused (distance) vision when lighting drops to low photopic and mesopic levels.[73,74] Balancing the need for expanded depth of field with the need to avoid loss of distance vision may require a small pupil approach that adjusts with light level, and this behaviour is generally observed with miotics drugs.[80] As pointed out by Charman,[21] effectiveness of expanding the eye's depth of field may also be enhanced if the eye is slightly myopic.

Lens mobility

Similar to the approach taken by some fish[7–9] and cats,[10] multifocality can also be achieved by adjusting the position of the eye's lens. This approach lies at the heart of strategies to re-establish accommodation in pseudophakic eyes. In particular, the Food and Drug Administration approved Crystalens (Bausch and Lomb, Rochester, NY, USA) employs a hinged haptic to try to utilise existing ciliary muscle activity to move the lens axially in pseudophakic eyes.[81] However, despite the addition of aspheric optics to the most recent lens design (Crystalens AO) aimed at creating spherical aberration-free surfaces,[82] inadequate axial movement has prevented this device from being widely successful.[83]

Lens power variations

Multifocality can also be achieved by non-dynamic methods. Similar to some fish,[15] optical corrections in which optical power varies with spatial location across the pupil have been implemented in modern multifocal IOLs[84–86] and contact lenses.[87–90] Radially symmetric or concentric design multifocal lenses are most common,[20] but early multifocal contact lenses employed a segmented geometry inherited from spectacle lenses,[91–93] as did the earliest bifocal IOL (a variant of which is still produced).[94] Segmented bifocal contact lenses, however, suffered from rotational instabilities,[92] and are now typically only implemented as gas-permeable lens designs utilised for a select patient group.[20] Optical modelling reveals, however, that meridionally segmented optical designs may offer superior optical performance.[95,96]

The core principle of a concentric multifocal design is that it will be rotationally insensitive and include two or more powers contained in geometrically separate zones located at different distances from the lens centre[97] (Figure 3). Designs that incorporate two powers in alternating annular zones often also include significant regions of the lens in which there is a gradual power change with increasing radial distance.[98,99] For example, in Figure 3, which shows high-resolution Shack-Hartmann two-dimensional power maps and radially averaged power profile maps, this can be seen in both the centre-distance (top left) and centre-near (lower left) designs, and to a lesser extent in the concentric ring design (top right). Manufacturing limitations may necessitate a spatial spread of the transition in optical power, thereby adding multiple powers, and thus authenticating 'multifocal' labelling despite the fact that the lens design may have been strictly bifocal. This manufacturing by-product is

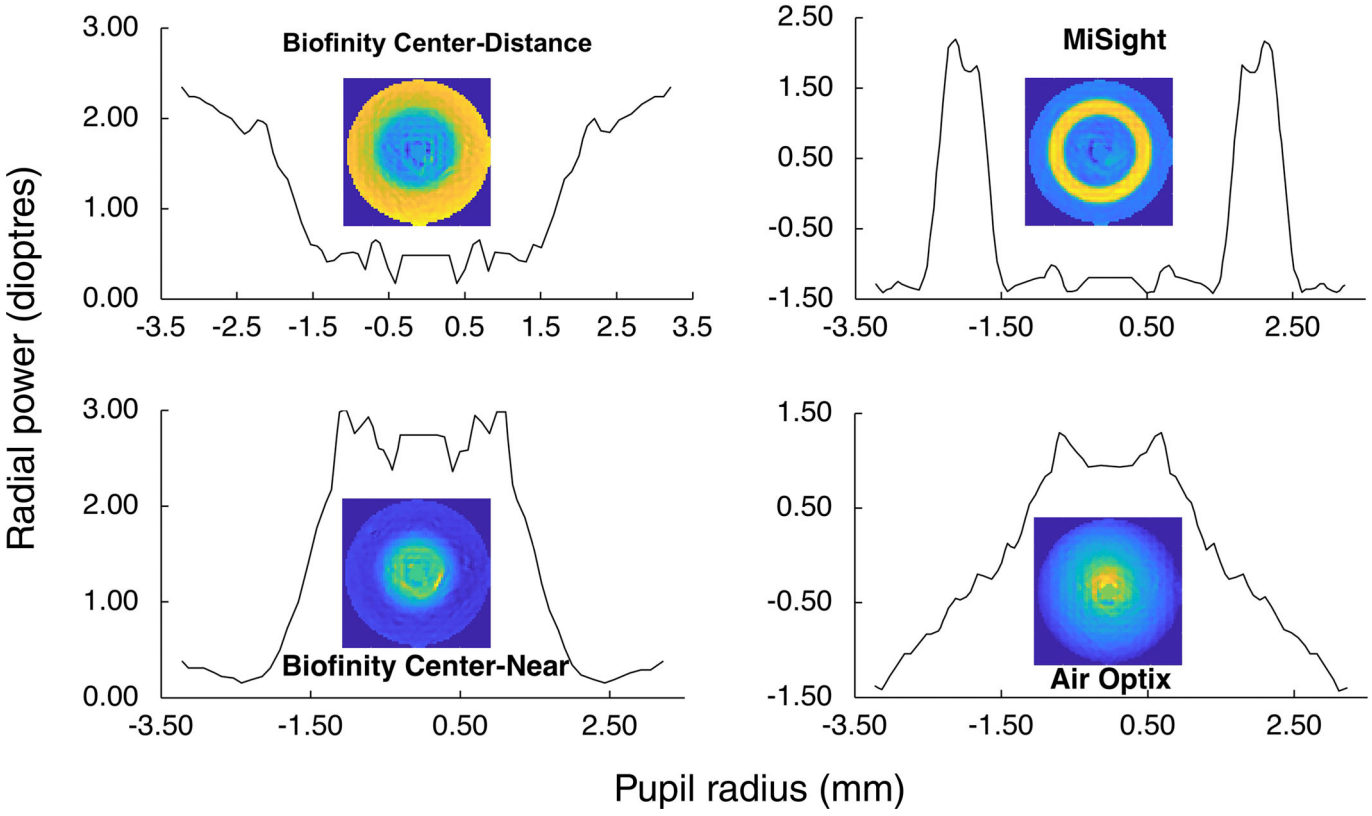

Figure 3. This figure shows power profiles of four multifocal contact lenses, two centre-distance designs (Biofinity CD and MiSight, both CooperVision, Pleasanton, CA, USA), and two centre-near designs (Biofinity CN and AirOptix, CooperVision and Alcon, Ltd, Fort Worth, TX, USA, respectively). Radial power was computed from wavefront slope data collected over a 7 mm analysis diameter (Power = slope/radius[178,179]) measured with a validated[129] Clear Wave (Lumetrics, Inc., Rochester, NY, USA) single pass Shack-Hartmann aberrometer (sample spacing of 0.104 mm). To avoid exaggerated computational noise errors near to the lens centre, power computations are not made in the central 0.6 mm, so this very centre data should be ignored. Colour maps show the radial symmetry of these four designs. In each colour map, the mean power is assigned green colour, and positive and negative deviations are coded by warm (yellow, orange) and cold (cyan, blue) colours, respectively.

quite different from a multifocal design containing a spatially extensive power gradient (similar to adding spherical aberration) from the lens centre to its periphery (Figure 3, lower right).

Another type of multifocal lens employs many concentric zones that each introduce half wavelength (or other fractional wavelength) optical path length steps between zones. These are usually referred to as diffractive lenses because their imaging properties rely on specific optical path length changes between zones[100,101] and result in constructive interference (images) at focal distances determined by the ring geometry.[102] In these lenses, a half wavelength (pi) phase shift between each zone produces a lens with two powers, a bifocal[26,101,103] and other phase step combinations can be used to generate trifocal designs.[104–106] These diffractive designs can be distinguished from the previously described concentric refractive lenses because every location across the lens contributes to each power, and thus these lenses are often referred to as 'full aperture' designs,[107–110] in which the relative amount of energy in the distance and near images does not necessarily vary with pupil size, as it does with concentric refracting designs.[97–99] Diffractive optics have been incorporated into several IOLs,[26,101,103,106,111,112] but have had limited commercial success as contact lenses (for example, Echelon[113,114] and Diffrax[115]).

The pupil size dependency of concentric refractive designs can be considered either a liability or an attractive feature of the design,[97] and indeed, several IOLs have specifically modified the standard diffractive design to generate a pupil size dependency in which the add optical power produced by the diffractive optical element contributes a higher proportion of the light in the image with small pupils and a much smaller proportion for large pupils. This 'centre-near' approach biases the optics toward the near add for near viewing (due to near viewing pupil miosis, which is present in older eyes[116,117]) but biases the optics to distance vision at night.[101,112] For example, a centre-near two-zone design with a central 3 mm diameter zone may become effectively a monofocal near correction at high light levels[97,98,118] resulting in all of the image energy being defocused when viewing distant objects. Similar to the diffractive lenses, an alternative design approach that varies power across meridians and not as a function of radius[95] may also have optical

characteristics that are approximately invariant as pupil size changes. Also, such designs avoid the inherently poor optical quality available from thin annular apertures[97] resulting in generally superior optical quality of the meridionally varying designs.[95] Such meridionally varying lenses were first introduced into IOLs by cementing together half lenses with differing powers.[94]

Eye's inherent multifocality

Although the presbyopic eye is often considered as a monofocal optical system to be augmented with multifocal lenses in presbyopia and pseudophakia, the eye's optics are actually multifocal. For example, ocular longitudinal chromatic aberration (LCA) of the human eye generates approximately a 2.5 D difference in refractive state at the two extremes of the visible spectrum. Whitefoot and Charman[119] examined the impact on depth of focus by doubling or correcting LCA. Depth of focus increased by 0.50 D when doubling LCA and decreased by 0.30 D when correcting LCA. Some diffractive lens designs have the opposite sign of longitudinal chromatic aberration to refractive optics (more power at long wavelength versus short).[102,103,115] Therefore, the reverse LCA in the first diffractive order used to contribute bifocal add power can mostly correct the ocular LCA,[103] providing improved polychromatic image quality. These studies reveal that the multifocality of human eyes due to the wavelength dependence of refractive index offers little true multifocality for polychromatic stimuli, as expected due to the large visual attenuation of the spectral margins.[120]

The human eye also exhibits significant multifocality at each wavelength, primarily due to spherical aberration and coma. The former produces optical power that varies with radius squared, typically resulting in a myopic shift of about 2.00 D at the edge of an 8 mm diameter pupil.[121] Coma, on the other hand, can create a meridional linear ramp of power across the pupil. Therefore, the typical eye has both inherent radial and meridional multifocality, but as most presbyopes can attest, these levels of inherent multifocality remain insufficient to provide the depth of focus required to navigate our three-dimensional world. However, the naturally occurring changes in refractive state across the pupil will add to (or subtract from) any multifocality provided by a contact lens or IOL.[97,122] Therefore, the significant positive spherical aberration exhibited by older eyes,[123–125] and the corneas of pseudophakes[126] may augment any centre-distance multifocal that also contributes more positive power with increasing radial distance from the lens centre (positive spherical aberration). However, in the case of centre-near designs which inherently contain negative spherical aberration,[27,98,99,122] ocular positive spherical aberration will subtract from the add power provided by the multifocal lens containing negative spherical aberration.[97] Importantly, ocular spherical aberration may be either a help or hindrance depending on the type of design being fit, and may likely contribute to the variable patient responses often experienced with these multifocal designs.[127] Therefore, to achieve a desired level of multifocality in the corrected eye requires larger radially varying power changes (spherical aberration) in the correcting lens of a centre-near design than of a centre-distance design.[27,97,122] Although it is a simple matter to add the extra radially varying power needed for the centre-near designs, high levels of spherical aberration in a contact lens will introduce more coma as the lens decentres,[128,129] a problem well documented in the contact lens[44,130–133] and IOL[134–140] literature. Because many commercially available multifocal contact lenses and IOLs employ centre-near designs this problem is likely to be commonplace.

Figure 4 quantifies this issue by examining the impact of lens decentration when the

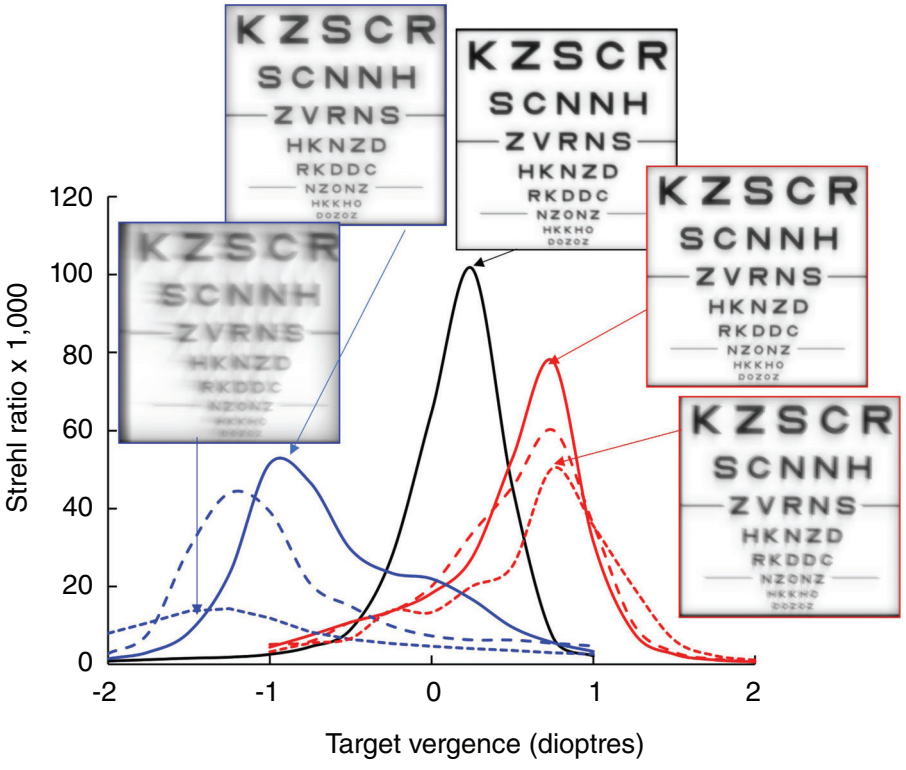

Figure 4. Impact on image quality of adding spherical aberration to achieve multifocality. The graph plots the Strehl Ratio image quality metric ×1,000 as a function of target vergence in dioptres for an aberrated presbyopic eye with a 6 mm pupil and +0.2 microns of C_4^0 (black curve), and for the same eye after spherical aberration has been added to give the eye+contact lens either +0.4 microns of C_4^0 spherical aberration (centre-distance model, red) or −0.4 microns of C_4^0 spherical aberration (centre-near model, blue). Further, 0.5 mm or 1.0 mm of lens decentration was introduced into the same centre-distance and centre-near models (dashed and dotted lines, respectively). Images of logMAR letter charts show the peak image quality achievable with and without 1 mm contact lens decentration.

added lens is designed to achieve a net spherical aberration level of 0.4 microns across a 6 mm pupil. The model included the reported higher-order aberrations of older eyes,[141] with a baseline spherical aberration level (C_4^0) of +0.2 microns. To achieve matching eye+lens resultant positive and negative multifocality levels of positive or negative (C_4^0) of 0.4 microns, the centre-distance lens must add +0.2 microns to the eye's +0.2 microns, but the centre-near lens must add −0.6 microns. The resulting peak image quality is slightly higher for the centre-distance model, but the impact of lens decentration is now much more dramatic for the centre-near model because the coma introduced by decentration scales with the magnitude of the spherical aberration levels within the contact lens.[128] Peak image quality (Figure 4, see inserts) and overall image quality ultimately is affected more by lens decentration in the centre-near design because of the higher levels of lens spherical aberration required to achieve multifocality.

Problem of the simultaneously present defocused images

Although zonal, diffractive bifocal, and multifocal lenses provide the different powers required to focus distance and near stimuli on the retina, the focused image is always coupled with a defocused image produced by the optical power inappropriate for the stimulus distance (for example, near optic and distant target). The amount of defocused light in a simple two-zone concentric design will vary systematically with pupil size[97,98,122] (Figure 5A). When the outer zone of a two-zone concentric design is defocused, the defocused point spread function will be an annulus.[97,142,143] In this case, the resulting annular 'halo' will increase in size as the pupil dilates and be most visible when the stimulus contrast is highest, as it is when viewing lights at night (a common source of visual disturbance clinically reported with multifocal optics). In addition to reducing the size of these haloes by reducing the add power (described as either low add multifocal lenses or 'extended depth of focus' lenses),[144] two alternative strategies have been proposed to minimise the visibility of these haloes. In one, the size of the defocused halo is reduced by coupling positive defocus with negative spherical aberration (that is,

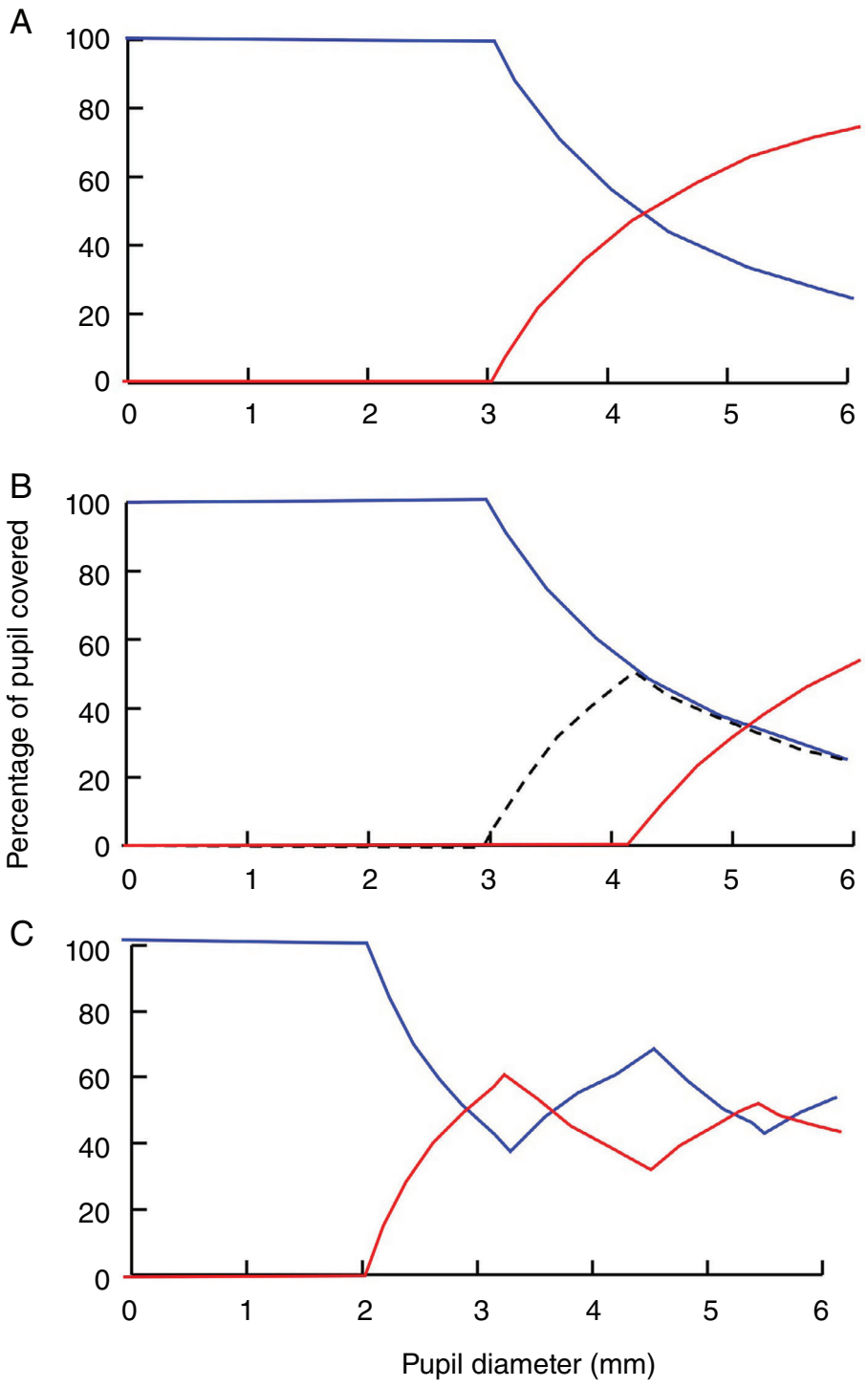

Figure 5. Three examples showing the relationship between pupil diameter (x-axis, mm) and the proportion of light imaged by each optic (y-axis) of radially varying zonal lenses. In each plot, the proportion of pupil covered by the distance (blue), near (red) and transition (black dashed) optics are plotted as a function of pupil diameter in mm for three centre-distance designs. Specifically, A: a lens with a 3 mm centre zone and an abrupt change to the add power, B: a centre-distance design with a 3 mm centre zone surrounded by 1.2 mm annulus across which power gradually changed to the near add power, and C: a five zone design with alternating distance (zones one, three, and five) and near (zones two and four) powers. Adapted from Bradley et al.[97] and Altoaimi et al.[98]

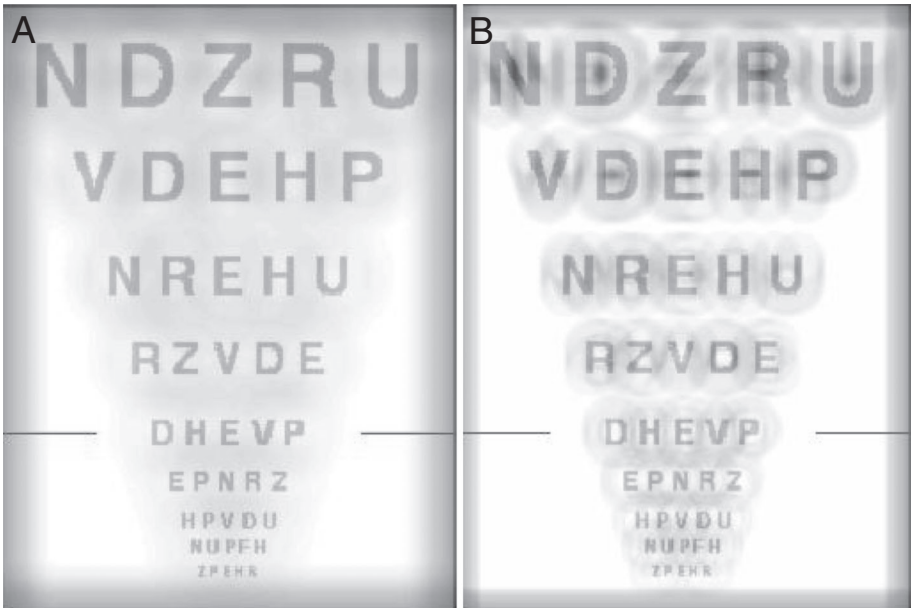

Figure 6. Simulated retinal images generated by a radially varying zonal bifocal lens when the centre zone is focused, and the add zone is nominally +2.00 D defocused. Centre zone diameter is 3 mm, pupil diameter is 6 mm. In A: 0.15 microns of positive spherical aberration was added to the add zone, and in B: negative spherical aberration was added.

including negative spherical aberration in the add zone) and vice versa. This produces a smaller but higher contrast halo. Alternatively, contrast of ghost images can be reduced by coupling positive spherical aberration with positive defocus (including positive spherical aberration in the add zone) and vice versa, which generates larger but lower contrast haloes with now clear edges.[145] The results of these two aberration-based strategies are simulated in Figure 6 for two designs of centre-distance optics with distance targets. On the left (Figure 6A), positive spherical aberration has been added to the near add zone increasing the size of the blur, but reducing its contrast, whereas on the right (Figure 6B), negative spherical aberration has been added to the add zone reducing the blur size but increasing its contrast. When positive defocus is generated by the add zone for distance stimuli, adding opposite sign negative spherical aberration creates high contrast phase reversed regions of the spatial frequency spectrum[103] which can disrupt the spatial structure of the focused image. This phase effect can be easily seen by comparing the phase correct but low contrast images in Figure 6A with the higher contrast but phase altered image in Figure 6B. Which would be more disruptive to a patient?

Adopting multifocal optical designs for the control of myopia

Although multifocal optical designs were originally developed to provide increased depth of focus for eyes lacking autofocus capability (presbyopic and pseudophakic eyes) as described above, recent experiments on infant monkeys have shown that adding some extra plus power to an otherwise hyperopic eye will slow the growth of the vitreal chamber resulting in reduced myopia.[146–148] Significantly, Smith et al. also showed that added plus power could be restricted to the peripheral retina and have a similar impact.[149] These two results have led to a rapid proliferation of optical interventions to control myopia development that employ added plus power, notably into the peripheral retina.[150–154] Plus power can be added to the peripheral retinal image using some of the same approaches described above, such as by several types of centre-distance concentric ring designs (for example, MiSight; CooperVision, Pleasanton, CA, USA) or annular (Biofinity Multifocal, CooperVision). The axial separation of the cornea and contact lens from the eye's entrance pupil necessitates that rays entering the pupil from the peripheral field must pass through the peripheral optics of the contact lens.[63,155–158] Of course, a similar variation in refractive state across the visual field may also potentially be created by aspheric lenses containing significant positive spherical aberration.[159] Likewise, orthokeratology also produces an eye with myopia in the peripheral optics or equivalently an eye with positive corneal plane spherical aberration.[27,160–162] Consistent with the hypothesis of removing peripheral hyperopia from the retinal image, these multifocal concentric ring[163] and annular[164–166] contact lens designs and the multifocal orthokeratology corneas have generally shown promise at slowing myopia development.[163,167–173]

Lessons from evolution

Evolution developed some of the multifocal strategies now used to correct presbyopia, and the need for improved surrogates for accommodation grows every day as the presbyopic population grows toward an estimated 1.8 billion by 2050.[174,175] Additionally, the value of multifocal optics has expanded due to its ability to slow myopia progression.[163,167–173] As work continues to optimise these designs, there may be as yet untried evolutionary strategies that can be adapted. The true long-term solution, and where much of our future research likely may need to occur may be in preventing the onset of presbyopia in the first place.[176] Or, better yet, maybe even preventing ageing from occurring in the first place?[177] However, until then, a key understanding of the strengths and limitations of accommodation surrogates and how they might be applied in our clinical practices to aid our patients is critical.

REFERENCES

1. Flitcroft DI. The complex interactions of retinal, optical and environmental factors in myopia aetiology. *Prog Retin Eye Res* 2012; 31: 622–660.
2. Hoffman DM, Banks MS. Focus information is used to interpret binocular images. *J Vis* 2010; 10: 13.
3. Thorn F, Schwartz F. Effects of dioptric blur on Snellen and grating acuity. *Optom Vis Sci* 1990; 67: 3–7.
4. Raviola E, Wiesel TN. Effect of dark-rearing on experimental myopia in monkeys. *Invest Ophthalmol Vis Sci* 1978; 17: 485–488.
5. Smith EL 3rd. Spectacle lenses and emmetropization: the role of optical defocus in regulating ocular development. *Optom Vis Sci* 1998; 75: 388–398.
6. Smith EL 3rd, Hung LF. The role of optical defocus in regulating refractive development in infant monkeys. *Vision Res* 1999; 39: 1415–1435.
7. Schwab IR, Dubielzig RR, Schobert C. *Evolution's Witness: How Eyes Evolved*. New York: Oxford University Press, 2012.

8. Schwab IR, Hart N. Cover illustration. More than black and white. *Br J Ophthalmol* 2006; 90: 406.
9. Khorramshahia O, Schartaua JM. Krogera RHH. A complex system of ligaments and a muscle keep the crystalline lens in place in the eyes of boy fishes (teleosts). *Vision Res* 2008; 48: 1503–1508.
10. Hughes A. Observing accommodation in the cat. *Vision Res* 1973; 13: 481–482.
11. Alevogt R, Alevogt R. Studien zur Kinematik der ChamaÈ leonzunge. *Z Vgl Physiol* 1954; 36: 66–77.
12. Flanders M. Visually guided head movement in the African chameleon. *Vision Res* 1985; 25: 935–942.
13. Kirmse W, Kirmse R, Milev E. Visuomotor operation in transition from object fixation to prey shooting in chameleons. *Biol Cybern* 1994; 71: 209–214.
14. Muntz WRA, Raj U. On the visual system of Nautilius Pompilius. *J Exp Biol* 1984; 109: 253–263.
15. Gagnon Y, Soderberg B, Kroger R. Optical advantages and function of multifocal spherical fish lenses. *J Opt Soc Am A Opt Image Sci Vis* 2012; 29: 1786–1793.
16. Ott M, Schaeffel F, Kirmse W. Binocular vision and accommodation in prey-catching chameleons. *J Comp Physiol A* 1998; 182: 319–330.
17. Duane A. An attempt to determine the normal range of accommodation at various ages, being a revision of Donder's experiments. *Trans Am Ophthalmol Soc* 1908; 11: 634–641.
18. Howland HC, Sivak JG. Penguin vision in air and water. *Vision Res* 1984; 24: 1905–1909.
19. Bito LZ, Kaufman PL, DeRousseau CJ et al. Presbyopia: an animal model and experimental approaches for the study of the mechanism of accommodation and ocular ageing. *Eye (Lond)* 1987; 1: 222–230.
20. Wolffsohn JS, Davies LN. Presbyopia: effectiveness of correction strategies. *Prog Retin Eye Res* 2019; 68: 124–143.
21. Charman WN. Pinholes and presbyopia: solution or sideshow? *Ophthalmic Physiol Opt* 2019; 39: 1–10.
22. Barrett BT, Bradley A, Candy TR. The relationship between anisometropia and amblyopia. *Prog Retin Eye Res* 2013; 36: 120–158.
23. Legras R, Hornain V, Monot A et al. Effect of induced anisometropia on binocular through-focus contrast sensitivity. *Optom Vis Sci* 2001; 78: 503–509.
24. Vandermeer G, Legras R, Gicquel JJ et al. Quality of vision with traditional monovision versus modified monovision. *Acta Ophthalmol Suppl* 2013; 91: S085.
25. Vandermeer G, Rio D, Gicquel JJ et al. Subjective through-focus quality of vision with various versions of modified monovision. *Br J Ophthalmol* 2015; 99: 997–1003.
26. Ravikumar S, Bradley A, Bharadwaj S et al. Expanding binocular depth of focus by combining monovision with diffractive bifocal intraocular lenses. *J Cataract Refract Surg* 2016; 42: 1288–1296.
27. Kollbaum PS. Optical aberrations of contact lenses and eyes corrected with contact lenses. In: *Optometry: Indiana University*. Bloomington, Indiana, 2007. pp. 196–233.
28. Schor C, Landsman L, Erickson P. Ocular dominance and the interocular suppression of blur in monovision. *Am J Optom Physiol Opt* 1987; 64: 723–730.
29. Fernandez EJ, Schwarz C, Prieto PM et al. Impact on stereo-acuity of two presbyopia correction approaches: monovision and small aperture inlay. *Biomed Opt Express* 2013; 4: 822–830.
30. Loshin DS. Binocular summation with monovision contact lens correction for presbyopia. *Int Contact Lens Clinic* 1982; 9: 161–173.
31. Collins M, Goode A, Brown B. Distance visual acuity and monovision. *Optom Vis Sci* 1993; 70: 723–728.
32. Lit A. Presentation of experimental data. *J Am Optom Assoc* 1968; 39: 1098–1099.
33. Westheimer G, McKee SP. Stereoscopic acuity with defocused and spatially filtered retinal images. *JOSA* 1980; 70: 772–778.
34. Back A, Grant T, Hine N. Comparative visual performance of three presbyopic contact lens corrections. *Optom Vis Sci* 1992; 69: 474–480.
35. Freeman MH, Charman WN. An exploration of modified monovision with diffractive bifocal contact lenses. *Cont Lens Anterior Eye* 2007; 30: 189–196.
36. Smith CE, Allison RS, Wilkinson F et al. Monovision: consequences for depth perception from large disparities. *Exp Eye Res* 2019; 183: 62–67.
37. Pollard ZF, Greenberg MF, Bordenca M et al. Strabismus precipitated by monovision. *Am J Ophthalmol* 2011; 152: 479–482 e471.
38. Legge GE, Rubin GS. Binocular interactions in suprathreshold contrast perception. *Percept Psychophys* 1981; 30: 49–61.
39. Ding J, Sperling G. A gain-control theory of binocular combination. *Proc Natl Acad Sci U S A* 2006; 103: 1141–1146.
40. Hickenbotham A, Tiruveedhula P, Roorda A. Comparison of spherical aberration and small-pupil profiles in improving depth of focus for presbyopic corrections. *J Cataract Refract Surg* 2012; 38: 2071–2079.
41. Xu R, Wang H, Jaskulski M et al. Small-pupil versus multifocal strategies for expanding depth of focus of presbyopic eyes. *J Cataract Refract Surg* 2019; 45: 647–655.
42. Smith G. Angular diameter of defocus blur discs. *Am J Optometry and Physiol Optics* 1982; 59: 885–889.
43. Winn B, Whitaker D, Elliott DB et al. Factors affecting light-adapted pupil size in normal human subjects. *Invest Ophthalmol Vis Sci* 1994; 35: 1132–1137.
44. Chateau N, De Brabander J, Bouchard F et al. Infrared pupillometry in presbyopes fitted with soft contact lenses. *Optom Vis Sci* 1996; 73: 733–741.
45. Xu R, Gil D, Dibas M et al. The effect of light level and small pupils on presbyopic reading performance. *Invest Ophthalmol Vis Sci* 2016; 57: 5656–5664.
46. Elliott SL, Choi SS, Doble N et al. Role of high-order aberrations in senescent changes in spatial vision. *J Vis* 2009; 9: 24.1–16.
47. Guirao A, Gonzalez C, Redondo M et al. Average optical performance of the human eye as a function of age in a normal population. *Invest Ophthalmol Vis Sci* 1999; 40: 203–213.
48. Pointer JS. The presbyopic add. I. Magnitude and distribution in a historical context. *Ophthalmic Physiol Opt* 1995; 15: 235–240.
49. Cheng X, Thibos LN, Bradley A. Estimating visual quality from wavefront aberration measurements. *J Refract Surg* 2003; 19: S579–S584.
50. Cheng X, Bradley A, Thibos LN. Predicting subjective judgment of best focus with objective image quality metrics. *J Vis* 2004; 4: 310–321.
51. Thibos LN, Hong X, Bradley A et al. Accuracy and precision of objective refraction from wavefront aberrations. *J Vis* 2004; 4: 329–351.
52. Kim WS, Park IK, Chun YS. Quantitative analysis of functional changes caused by pinhole glasses. *Invest Ophthalmol Vis Sci* 2014; 55: 6679–6685.
53. Kim WS, Park IK, Park YK et al. Comparison of objective and subjective changes induced by multiple-pinhole glasses and single-pinhole glasses. *J Korean Med Sci* 2017; 32: 850–857.
54. Wittenberg S. Pinhole eyewear systems: a special report. *J Am Optom Assoc* 1993; 64: 112–116.
55. Dick HB. Small-aperture strategies for the correction of presbyopia. *Curr Opin Ophthalmol* 2019; 30: 236–242.
56. Seyeddain O, Hohensinn M, Riha W et al. Small-aperture corneal inlay for the correction of presbyopia: 3-year follow-up. *J Cataract Refract Surg* 2012; 38: 35–45.
57. Srinivasan S. Small aperture intraocular lenses: the new kids on the block. *J Cataract Refract Surg* 2018; 44: 927–928.
58. Campos M, Beer S, Nakano EM et al. Complete depigmentation of a small aperture corneal inlay implanted for compensation of presbyopia. *Arq Bras Oftalmol* 2017; 80: 52–56.
59. GOt W. Correction of presbyopia with a small aperture corneal inlay. *J Refract Surg* 2011; 27: 842–845.
60. Dexl AK, Seyeddain O, Riha W et al. Reading performance after implantation of a small-aperture corneal inlay for the surgical correction of presbyopia: two-year follow-up. *J Cataract Refract Surg* 2011; 37: 525–531.
61. Freeman E. Pinhole contact lenses. *Am J Optom Arch Am Acad Optom* 1952; 29: 347–352.
62. Albarran Diego C, Montes-Mico R, Pons AM et al. Influence of the luminance level on visual performance with a disposable soft cosmetic tinted contact lens. *Ophthalmic Physiol Opt* 2001; 21: 411–419.
63. Atchison DA, Blazaki S, Suheimat M et al. Do small-aperture presbyopic corrections influence the visual field? *Ophthalmic Physiol Opt* 2016; 36: 51–59.
64. Langenbucher A, Goebels S, Szentmary N et al. Vignetting and field of view with the KAMRA corneal inlay. *Biomed Res Int* 2013; 2013: 154593.
65. Nau A. A contact lens model to produce reversible visual field loss in healthy subjects. *J Am Optom Assoc* 2012; 83: 279–284.
66. Carkeet A. Field restriction and vignetting in contact lenses with opaque peripheries. *Clin Exp Optom* 1998; 81: 151–158.
67. Renna A, Alio JL, Vejarano LF. Pharmacological treatments of presbyopia: a review of modern perspectives. *Eye Vis (Lond)* 2017; 4: 3.
68. Abdelkader A. Improved presbyopic vision with miotics. *Eye Contact Lens* 2015; 41: 323–327.
69. Abdelkader A, Kaufman HE. Clinical outcomes of combined versus separate carbachol and brimonidine drops in correcting presbyopia. *Eye Vis (Lond)* 2016; 3: 31.
70. Benozzi J, Benozzi G, Orman B. Presbyopia: a new potential pharmacological treatment. *Med Hypothesis Discov Innov Ophthalmol* 2012; 1: 3–5.
71. Dick HB, Piovella M, Vukich J et al. Prospective multicenter trial of a small-aperture intraocular lens in cataract surgery. *J Cataract Refract Surg* 2017; 43: 956–968.
72. Trindade C. Small aperture (pinhole) intraocular implant to increase depth of focus. In: *Application UP ed. US*, 2014.
73. Xu R, Wang H, Thibos LN et al. Interaction of aberrations, diffraction, and quantal fluctuations determine the impact of pupil size on visual quality. *J Opt Soc Am A Opt Image Sci Vis* 2017; 34: 481–492.
74. Xu R, Thibos L, Bradley A. Effect of target luminance on optimum pupil diameter for presbyopic eyes. *Optom Vis Sci* 2016; 93: 1409–1419.
75. Van Nes F, Baouman M. Spatial modulation transfer in the human eye. *JOSA* 1967; 57: 401–406.
76. Banks MS, Geisler WS, Bennett PJ. The physical limits of grating visibility. *Vision Res* 1987; 27: 1915–1924.
77. Campbell FW, Gregory AH. Effect of size of pupil on visual acuity. *Nature* 1960; 187: 1121–1123.
78. Woodhouse JM. The effect of pupil size on grating detection at various contrast levels. *Vision Res* 1975; 15: 645–648.
79. Seyeddain O, Riha W, Hohensinn M et al. Refractive surgical correction of presbyopia with the AcuFocus small aperture corneal inlay: two-year follow-up. *J Refract Surg* 2010; 26: 707–715.
80. McDonald JE 2nd, El-Moatassem Kotb AM, Decker BB. Effect of brimonidine tartrate ophthalmic solution 0.2% on pupil size in normal eyes under different luminance conditions. *J Cataract Refract Surg* 2001; 27: 560–564.
81. Marchini G, Pedrotti E, Sartori P et al. Ultrasound biomicroscopic changes during accommodation in eyes with accommodating intraocular lenses: pilot study and hypothesis for the mechanism of accommodation. *J Cataract Refract Surg* 2004; 30: 2476–2482.
82. Incorporated BaL. Bausch and Lomb Crystalens Accommodating Posterior Chamber Intraocular Lens Device Description. [Cited 07 Jan 2019] Available at: https://www.bausch.com/ecp/our-products/cataract-surgery/lens-systems/crystalens-ao, 2016.
83. Marcos S, Ortiz S, Perez-Merino P et al. Three-dimensional evaluation of accommodating intraocular lens shift and alignment in vivo. *Ophthalmology* 2014; 121: 45–55.
84. McNeely RN, Pazo E, Spence A et al. Visual quality and performance comparison between 2 refractive rotationally asymmetric multifocal intraocular lenses. *J Cataract Refract Surg* 2017; 43: 1020–1026.

85. Tan N, Zheng D, Ye J. Comparison of visual performance after implantation of 3 types of intraocular lenses: accommodative, multifocal, and monofocal. *Eur J Ophthalmol* 2014; 24: 693–698.
86. Lane SS, Morris M, Nordan L et al. Multifocal intraocular lenses. *Ophthalmol Clin North Am* 2006; 19: 89–105 vi.
87. Legras R, Rio D. Simulation of commercial vs theoretically optimised contact lenses for presbyopia. *Ophthalmic Physiol Opt* 2017; 37: 297–304.
88. Monsalvez-Romin D, Dominguez-Vicent A, Garcia-Lazaro S et al. Power profiles in multifocal contact lenses with variable multifocal zone. *Clin Exp Optom* 2018; 101: 57–63.
89. Kim E, Bakaraju RC, Ehrmann K. Power profiles of commercial multifocal soft contact lenses. *Optom Vis Sci* 2017; 94: 183–196.
90. Wagner S, Conrad F, Bakaraju RC et al. Power profiles of single vision and multifocal soft contact lenses. *Cont Lens Anterior Eye* 2015; 38: 2–14.
91. Robboy M, Erickson P. Performance comparison of current hydrophilic alternating vision bifocal contact lenses. *Int Contact Lens Clinic* 1987; 14: 237–243.
92. Borish IM, Soni S. Bifocal contact lenses. *J Am Optom Assoc* 1982; 53: 219–229.
93. Toshida H, Takahashi K, Sado K et al. Bifocal contact lenses: history, types, characteristics, and actual state and problems. *Clin Ophthalmol* 2008; 2: 869–877.
94. Hoffer KJ, Savini G. Multifocal intraocular lenses: historical perspective. In: Alió JL, Joseph P, eds. *Multifocal Intraocular Lenses: The Art and the Practice, Essentials in Ophthalmology*. Switzerland: Springer, 2014. pp. 5–28.
95. de Gracia P, Hartwig A. Optimal orientation for angularly segmented multifocal corrections. *Ophthalmic Physiol Opt* 2017; 37: 610–623.
96. de Gracia P, Dorronsoro C, Marcos S. Multiple zone multifocal phase designs. *Opt Lett* 2013; 38: 3526–3529.
97. Bradley A, Nam J, Xu R et al. Impact of contact lens zone geometry and ocular optics on bifocal retinal image quality. *Ophthalmic Physiol Opt* 2014; 34: 331–345.
98. Altoaimi BH, Kollbaum P, Meyer D et al. Experimental investigation of accommodation in eyes fit with multifocal contact lenses using a clinical auto-refractor. *Ophthalmic Physiol Opt* 2018; 38: 152–163.
99. Plainis S, Atchison DA, Charman WN. Power profiles of multifocal contact lenses and their interpretation. *Optom Vis Sci* 2013; 90: 1066–1077.
100. Klein SA. Understanding the diffractive bifocal contact lens. *Optom Vis Sci* 1993; 70: 439–460.
101. Davison JA, Simpson MJ. History and development of the apodized diffractive intraocular lens. *J Cataract Refract Surg* 2006; 32: 849–858.
102. Buralli D, Morris G, Rogers J. Optical performance of holographic kinoforms. *Appl Optics* 1989; 28: 976–983.
103. Ravikumar S, Bradley A, Thibos LN. Chromatic aberration and polychromatic image quality with diffractive multifocal intraocular lenses. *J Cataract Refract Surg* 2014; 40: 1192–1204.
104. Lee S, Choi M, Xu Z et al. Optical bench performance of a novel trifocal intraocular lens compared with a multifocal intraocular lens. *Clin Ophthalmol* 2016; 10: 1031–1038.
105. Alio JL, Plaza-Puche AB, Alio Del Barrio JL et al. Clinical outcomes with a diffractive trifocal intraocular lens. *Eur J Ophthalmol* 2018; 28: 419–424.
106. Cochener B, Boutillier G, Lamard M et al. A comparative evaluation of a new generation of diffractive trifocal and extended depth of focus intraocular lenses. *J Refract Surg* 2018; 34: 507–514.
107. Barton K, Freeman MH, Woodward EG et al. Diffractive bifocal contact lenses in aphakia and pseudophakia. *A pilot study Eye (Lond)* 1991; 5: 344–347.
108. Schwiegerling J. Analysis of the optical performance of presbyopia treatments with the defocus transfer function. *J Refract Surg* 2007; 23: 965–971.
109. Choi J, Schwiegerling J. Optical performance measurement and night driving simulation of ReSTOR, ReZoom, and Tecnis multifocal intraocular lenses in a model eye. *J Refract Surg* 2008; 24: 218–222.
110. Zheleznyak L, Kim MJ, MacRae S et al. Impact of corneal aberrations on through-focus image quality of presbyopia-correcting intraocular lenses using an adaptive optics bench system. *J Cataract Refract Surg* 2012; 38: 1724–1733.
111. Simpson MJ. Re: assessing the optical performance of multifocal (diffractive) intraocular lenses. *Ophthalmic Physiol Opt* 2009; 29: 207.
112. Simpson MJ. Diffractive multifocal intraocular lens image quality. *Appl Optics* 1992; 31: 3621–3626.
113. Atchison DA, Ye M, Bradley A et al. Chromatic aberration and optical power of a diffractive bifocal contact lens. *Optom Vis Sci* 1992; 69: 797–804.
114. Bradley A, Abdul Rahman H, Soni PS et al. Effects of target distance and pupil size on letter contrast sensitivity with simultaneous vision bifocal contact lenses. *Optom Vis Sci* 1993; 70: 476–481.
115. Freeman M, Stone J. A new diffractive bifocal contact lens. *Trans BCLA* 1987; 10: 15–22.
116. Radhakrishnan H, Charman WN. Age-related changes in static accommodation and accommodative miosis. *Ophthalmic Physiol Opt* 2007; 27: 342–352.
117. Altoaimi BH, Almutairi MS, Kollbaum P et al. Accommodative behavior of eyes wearing aspheric single vision contact lenses. *Optom Vis Sci* 2017; 94: 971–980.
118. Charman WN, Radhakrishnan H. Accommodation, pupil diameter and myopia. *Ophthalmic Physiol Opt* 2009; 29: 72–79.
119. Whitefoot HD, Charman WN. Hyperchromatic lenses as potential aids for the presbyope. *Ophthalmic Physiol Opt* 1995; 15: 13–22.
120. Bradley A, Glenn A. Fry Award Lecture 1991: perceptual manifestations of imperfect optics in the human eye: attempts to correct for ocular chromatic aberration. *Optom Vis Sci* 1992; 69: 515–521.
121. Thibos LN, Ye M, Zhang X et al. Spherical aberration of the reduced schematic eye with elliptical refracting surface. *Optom Vis Sci* 1997; 74: 548–556.
122. Kollbaum PS, Bradley A, Thibos LN. Comparing the optical properties of soft contact lenses on and off the eye. *Optom Vis Sci* 2013; 90: 924–936.
123. Guirao A, Redondo M, Artal P. Optical aberrations of the human cornea as a function of age. *J Opt Soc Am A Opt Image Sci Vis* 2000; 17: 1697–1702.
124. Artal P, Berrio E, Guirao A et al. Contribution of the cornea and internal surfaces to the change of ocular aberrations with age. *J Opt Soc Am A Opt Image Sci Vis* 2002; 19: 137–143.
125. Brunette I, Bueno JM, Harissi-Dagher M et al. Optical quality of the eye with the Artisan phakic lens for the correction of high myopia. *Optom Vis Sci* 2003; 80: 167–174.
126. Wang L, Santaella RM, Booth M et al. Higher-order aberrations from the internal optics of the eye. *J Cataract Refract Surg* 2005; 31: 1512–1519.
127. Bakaraju RC, Ehrmann K, Ho A et al. Inherent ocular spherical aberration and multifocal contact lens optical performance. *Optom Vis Sci* 2010; 87: 1009–1022.
128. Guirao A, Williams DR, Cox IG. Effect of rotation and translation on the expected benefit of an ideal method to correct the eye's higher-order aberrations. *J Opt Soc Am A Opt Image Sci Vis* 2001; 18: 1003–1015.
129. Kollbaum P, Jansen M, Thibos L et al. Validation of an off-eye contact lens Shack-Hartmann wavefront aberrometer. *Optom Vis Sci* 2008; 85: E817–E828.
130. Belda-Salmeron L, Drew T, Hall L et al. Objective analysis of contact lens fit. *Cont Lens Anterior Eye* 2015; 38: 163–167.
131. Woods RL, Saunders JE, Port MJ. Optical performance of decentered bifocal contact lenses. *Optom Vis Sci* 1993; 70: 171–184.
132. Wake E, Tienda JB, Uyekawa PM et al. Centration and coverage of hydrogel contact lenses. *Am J Optom Physiol Opt* 1981; 58: 302–308.
133. Mackie IA, Mason D, Perry BJ. Factors influencing corneal contact lens centration. *Br J Physiol Opt* 1970; 25: 87–103.
134. Holladay JT, Calogero D, Hilmantel G et al. Special report: American academy of ophthalmology task force summary statement for measurement of tilt, decentration, and chord length. *Ophthalmology* 2017; 124: 144–146.
135. Monestam E. Frequency of intraocular lens dislocation and pseudophacodonesis, 20 years after cataract surgery - a prospective study. *Am J Ophthalmol* 2019; 198: 215–222.
136. Perez-Merino P, Marcos S. Effect of intraocular lens decentration on image quality tested in a custom model eye. *J Cataract Refract Surg* 2018; 44: 889–896.
137. Schroder S, Schrecker J, Daas L et al. Impact of intraocular lens displacement on the fixation axis. *J Opt Soc Am A Opt Image Sci Vis* 2018; 35: 561–566.
138. Uzel MM, Ozates S, Koc M et al. Decentration and tilt of intraocular lens after posterior capsulotomy. *Semin Ophthalmol* 2018; 33: 766–771.
139. Zhu X, He W, Zhang Y et al. Inferior decentration of multifocal intraocular lenses in myopic eyes. *Am J Ophthalmol* 2018; 188: 1–8.
140. Zhu X, Zhang Y, He W et al. Tilt, decentration, and internal higher-order aberrations of sutured posterior-chamber intraocular lenses in patients with open globe injuries. *J Ophthalmol* 2017; 2017: 3517461.
141. Wang L, Koch DD. Ocular higher-order aberrations in individuals screened for refractive surgery. *J Cataract Refract Surg* 2003; 29: 1896–1903.
142. Charman WN. Theoretical aspects of concentric varifocal lenses. *Ophthalmic Physiol Opt* 1982; 2: 75–86.
143. Charman WN, Murray IJ, Nacer M et al. Theoretical and practical performance of a concentric bifocal intraocular implant lens. *Vision Res* 1998; 38: 2841–2853.
144. Gatinel D, Loicq J. Clinically relevant optical properties of bifocal, trifocal, and extended depth of focus intraocular lenses. *J Refract Surg* 2016; 32: 273–280.
145. Bradley A, Kollbaum PS, Thibos LN. Multifocal correction providing improved quality of vision. In: *USPTO ed. United States*, 2012.
146. Arumugam B, Hung LF, To CH et al. The effects of simultaneous dual focus lenses on refractive development in infant monkeys. *Invest Ophthalmol Vis Sci* 2014; 55: 7423–7432.
147. Arumugam B, Hung LF, To CH et al. The effects of the relative strength of simultaneous competing defocus signals on emmetropization in infant rhesus monkeys. *Invest Ophthalmol Vis Sci* 2016; 57: 3949–3960.
148. Smith EL 3rd, Hung LF, Huang J et al. Effects of local myopic defocus on refractive development in monkeys. *Optom Vis Sci* 2013; 90: 1176–1186.
149. Smith EL 3rd, Ramamirtham R, Qiao-Grider Y et al. Effects of foveal ablation on emmetropization and form-deprivation myopia. *Invest Ophthalmol Vis Sci* 2007; 48: 3914–3922.
150. Mutti DO, Sinnott LT, Reuter KS et al. Peripheral refraction and eye lengths in myopic children in the bifocal lenses in nearsighted kids (BLINK) study. *Transl Vis Sci Technol* 2019; 8: 17.
151. Liu Y, Wildsoet C. The effect of two-zone concentric bifocal spectacle lenses on refractive error development and eye growth in young chicks. *Invest Ophthalmol Vis Sci* 2011; 52: 1078–1086.
152. Charman WN, Mountford J, Atchison DA et al. Peripheral refraction in orthokeratology patients. *Optom Vis Sci* 2006; 83: 641–648.
153. Smith EL 3rd, Hung LF, Huang J. Relative peripheral hyperopic defocus alters central refractive development in infant monkeys. *Vision Res* 2009; 49: 2386–2392.
154. Shen J, Clark CA, Soni PS et al. Peripheral refraction with and without contact lens correction. *Optom Vis Sci* 2010; 87: 642–655.
155. Almutleb ES, Bradley A, Jedlicka J et al. Simulation of a central scotoma using contact lenses with an opaque centre. *Ophthalmic Physiol Opt* 2018; 38: 76–87.

156. Fedtke C, Manns F, Ho A. The entrance pupil of the human eye: a three-dimensional model as a function of viewing angle. *Opt Express* 2010; 18: 22364–22376.
157. Mathur A, Gehrmann J, Atchison DA. Pupil shape as viewed along the horizontal visual field. *J Vis* 2013; 13: 3.
158. Spring KH, Apparent Shape SWS. Size of the pupil viewed obliquely. *Br J Ophthalmol* 1948; 32: 347–354.
159. Cheng X, Xu J, Chehab K et al. Soft contact lenses with positive spherical aberration for myopia control. *Optom Vis Sci* 2016; 93: 353–366.
160. Hiraoka T, Matsumoto Y, Okamoto F et al. Corneal higher-order aberrations induced by overnight orthokeratology. *Am J Ophthalmol* 2005; 139: 429–436.
161. Hiraoka T, Okamoto C, Ishii Y et al. Contrast sensitivity function and ocular higher-order aberrations following overnight orthokeratology. *Invest Ophthalmol Vis Sci* 2007; 48: 550–556.
162. Gifford P, Li M, Lu H et al. Corneal versus ocular aberrations after overnight orthokeratology. *Optom Vis Sci* 2013; 90: 439–447.
163. Chamberlain P, Peixoto-de-Matos P, Logan NS et al. A three-year randomized clinical trial of misight lenses for myopia control. *Optom Vis Sci* 2019; 96: 556–567.
164. Smith MJ, Walline JJ. Controlling myopia progression in children and adolescents. *Adolesc Health Med Ther* 2015; 6: 133–140.
165. Walline JJ, Greiner KL, McVey ME et al. Multifocal contact lens myopia control. *Optom Vis Sci* 2013; 90: 1207–1214.
166. Walline JJ, Lindsley K, Vedula SS et al. Interventions to slow progression of myopia in children. *Cochrane Database Syst Rev* 2011: CD004916.
167. Cho P, Cheung SW, Edwards M. The longitudinal orthokeratology research in children (LORIC) in Hong Kong: a pilot study on refractive changes and myopic control. *Curr Eye Res* 2005; 30: 71–80.
168. Walline JJ, Jones LA, Sinnott LT. Corneal reshaping and myopia progression. *Br J Ophthalmol* 2009; 93: 1181–1185.
169. Kakita T, Hiraoka T, Oshika T. Influence of overnight orthokeratology on axial elongation in childhood myopia. *Invest Ophthalmol Vis Sci* 2011; 52: 2170–2174.
170. Santodomingo-Rubido J, Villa-Collar C, Gilmartin B et al. Myopia control with orthokeratology contact lenses in Spain: refractive and biometric changes. *Invest Ophthalmol Vis Sci* 2012; 53: 5060–5065.
171. Cho P, Cheung SW. Retardation of myopia in Orthokeratology (ROMIO) study: a 2-year randomized clinical trial. *Invest Ophthalmol Vis Sci* 2012; 53: 7077–7085.
172. Hiraoka T, Kakita T, Okamoto F et al. Long-term effect of overnight orthokeratology on axial length elongation in childhood myopia: a 5-year follow-up study. *Invest Ophthalmol Vis Sci* 2012; 53: 3913–3919.
173. Charm J, Cho P. High myopia-partial reduction ortho-k: a 2-year randomized study. *Optom Vis Sci* 2013; 90: 530–539.
174. Holden BA, Fricke TR, Ho SM et al. Global vision impairment due to uncorrected presbyopia. *Arch Ophthalmol* 2008; 126: 1731–1739.
175. Frick KD, Joy SM, Wilson DA et al. The global burden of potential productivity loss from uncorrected presbyopia. *Ophthalmology* 2015; 122: 1706–1710.
176. Tsuneyoshi Y, Higuchi A, Negishi K et al. Suppression of presbyopia progression with pirenoxine eye drops: experiments on rats and non-blinded, randomized clinical trial of efficacy. *Sci Rep* 2017; 7: 6819.
177. Lai RW, Lu R, Danthi PS et al. Multi-level remodeling of transcriptional landscapes in aging and longevity. *BMB Rep* 2019; 52: 86–108.
178. Southwell WH. Wave-front estimation from wave-front slope measurements. *J Opt Soc Am* 1980; 70: 998–1006.
179. Himebaugh NL, Nam J, Bradley A et al. Scale and spatial distribution of aberrations associated with tear breakup. *Optom Vis Sci* 2012; 89: 1590–1600.